PHYSICAL PROPERTIES OF WOOD – BASED CARBON MONOLITHS

Alain Celzard[1], Olaf Treusch[2], Jean-François Marêché[1], Gerd Wegener[2]
[1]*Laboratoire de Chimie du Solide Minéral, Université Henri Poincaré - Nancy I, UMR - CNRS 7555, BP 239, 54506 Vandoeuvre-lès-Nancy, France*
[2]*Technische Universität München, Holzforschung München, Winzererstr. 45, 80797 München, Germany*

Corresponding author e-mail address:Alain.Celzard@lcsm.uhp-nancy.fr

Introduction

Percolation and effective-medium theories (PT and EMT, respectively) are actually known to be very powerful tools of investigating various phenomena in heterogeneous materials. Both theories were indeed already applied to a large number of different model materials, mainly for confirming theoretical predictions. Recently, it was shown that the physical properties of many carbonaceous materials were accurately accounted for by PT and EMT, and that very important structural information could be derived from their application. Especially, composite materials based on dispersed graphite flakes or carbon fibres [1], carbonised anthracites [2], carbon powders [3,4] and compressed expanded graphite [5-8] were suitably described through these two theories.

In the present work, new monolithic carbonaceous wood-based materials were investigated by electrical conductivity measurements and by determining their elastic modulus. For both properties evidences of percolation behaviour were found. Applying PT and EMT, the morphological characteristics of both the solid and the pore phases were derived, as well as the nature of the mechanical contacts between the constituting carbon grains. Finally, the relationship between conductivity and rigidity thresholds was established.

Experimental

Wood-based composites were made by mixing wood fibres with 10 % of a powdery phenolic resin (Bakelite) in a stirring device. Subsequently the mixture was pressed to form boards of 10 mm thickness and densities from 0.3 to 1.2 g cm^{-3} in a uni-axial pressing process at a temperature of 180 °C. The fibreboards were dried at 103 °C for 2 h, and their carbonisation was carried out in an inert atmosphere (N_2). To make sure that the carbon materials remained crack-free, a slow heating rate of 1 K/min was applied up to 500 °C. A heating rate of 5 K/min was applied up to the peak temperature of 900 °C, which was kept for 2 h.

SEM pictures of the monolithic materials evidenced that the fibre-like particles are randomly disordered and entangled with each other. The monoliths are then, macroscopically speaking, perfectly homogeneous and exhibit no anisotropy.

Additionally, they are crack-free, thus allowing the measurement of both their conducting and elastic properties. Uncompacted wood fibres were pyrolized in the same conditions as those already used for the monoliths (i.e., up to 900 °C according to the heating rate detailed above). Fig. 1 shows the wood fibres (a) before and (b) after carbonisation. Most of the particles have lengths being typically slightly below 300 µm and diameters close to 30 µm, leading to an average ratio length to diameter close to 10. Carbonising the fibres does not seem to have much effect on their morphology, since Fig. 1(a) and 1(b) are very similar.

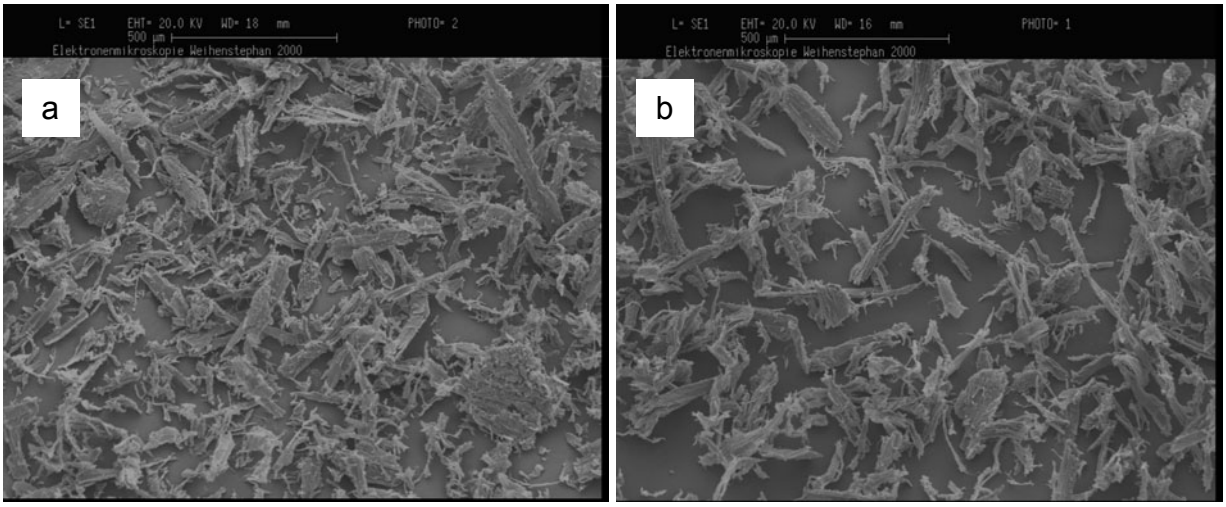

Figure 1. SEM pictures of (a) the crude and (b) the carbonised wood fibres.

For electrical conductivity measurements, parallelepipedic samples were cut. The smallest opposite faces were covered with silver paint, with which two copper wires were glued to each surface. The electrical conductivity was then measured according to the 4-probe method. Elastic moduli of the wood-based carbon materials were determined by three point bending tests according to the german industrial standard DIN 51902. Eight samples per density range were tested with a universal testing apparatus (TesT 112.50kn.L) at room temperature.

Results and Discussion

Electrical conductivity

The conductivity of the monoliths, σ_m, plotted versus the volume fraction Φ of carbon grains within the monoliths is presented in Fig. 2. Φ was calculated as the ratio d/d_{wf}, where d is the density of each monolithic material, and d_{wf} that of a typical carbonised wood fibre such that $d_{wf} \approx 1.39$ g cm^{-3}. The plot clearly shows the existence of a non-zero critical content Φ_c, i.e., a percolation threshold, at which σ_m vanishes. Above but near Φ_c, PT predicts that the conductivity reads [9-11] :

$$\sigma_m = \sigma_h \left(\Phi - \Phi_c\right)^t . \qquad (1)$$

In Eq. (1), σ_h is the intrinsic conductivity of the carbon particles, and t is the percolation conductivity critical exponent. For classical 3D systems, t is usually close to 2 [9,12].

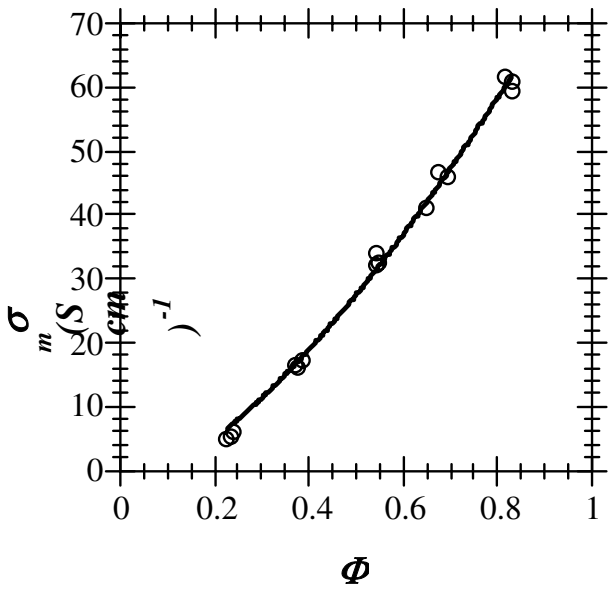

Figure 2. Electrical conductivity (σ_m) vs the volume fraction (Φ) of carbon particles. The solid curve is calculated with Eq. (3).

The data $\sigma_m(\Phi)$ may be studied in the framework of EMT, for which each grain of a binary mixture is surrounded by an average medium possessing the effective conductivity of the composite material itself. The general effective media (GEM) equation describes a binary disordered medium in which neither the grains of the two phases are mixed together on a symmetric basis, nor one phase completely coats the other. It reads [13,14] :

$$(1-\Phi)\frac{\sigma_l^{1/t'}-\sigma_m^{1/t'}}{\sigma_l^{1/t'}+\frac{1-\Phi_c}{\Phi_c}\sigma_m^{1/t'}}+\Phi\frac{\sigma_h^{1/t'}-\sigma_m^{1/t'}}{\sigma_h^{1/t'}+\frac{1-\Phi_c}{\Phi_c}\sigma_m^{1/t'}}=0 \qquad (2)$$

where σ_l is the conductivity of the low-conductivity phase (the air), and σ_h that of the high-conductivity phase (the carbon). t' is an exponent related both to the critical volume fraction Φ_c and to the shape of the grains. In the case of porous monoliths, i.e., mixtures of conducting grains and air, $\sigma_l = 0$ and hence Eq. (2) reduces to :

$$\sigma_m = \sigma_h \left(\frac{\Phi-\Phi_c}{1-\Phi_c}\right)^{t'} . \qquad (3)$$

This formula has the same form as the percolation Eq. (1). Nevertheless, while the percolation exponent t was only expected to take universal values depending on the dimensionality of the system, t' may be found in a wider range of values and reads [15] :

$$t' = m_h\,\Phi_c = m_l\,(1-\Phi_c) = \frac{m_l\,m_h}{m_l+m_h} . \qquad (4)$$

Eq. (4) holds if both phases are randomly oriented ellipsoidal grains having semiaxes $a = b \neq c$; then, the coefficients m_h and m_l satisfy the following equations [3,16] :

$$m_h = \frac{1 + 3L_h^{\,c}}{3L_h^{\,c}\left(1 - L_h^{\,c}\right)}$$
$$m_l = \frac{5 - 3L_l^{\,c}}{3\left(1 - L_l^{\,c\,2}\right)} \quad . \tag{5}$$

$L_{h(l)}^{\,c}$ denote the effective depolarisation factors of the high- (low-) conductivity phases associated with the principal axis (*c*) of the ellipsoids, and are directly linked to the shape of the grains. Indeed, the eccentricity *e* of the ellipsoids and their corresponding depolarisation factors L^c are written as [17] :

$$\text{prolate ellipsoids } (a/c < 1): \quad e = \sqrt{1 - (a/c)^2}, \quad L^c = \frac{1 - e^2}{2e^3}\ln\frac{1+e}{1-e} - 2e \tag{6a}$$

$$\text{oblate ellipsoids } (a/c > 1): \quad e = \sqrt{(a/c)^2 - 1}, \quad L^c = \frac{1 + e^2}{e^3}[e - \arctan e] \tag{6b}$$

In each case, spherical grains (*a* = *b* = *c*) leads to $e \to 0$ and $L^c \to 1/3$. Therefore m_h and m_l take their minimum values 3 and 3/2, respectively. If the aspect ratio *a*/*c* vanishes, i.e., corresponding to fibres or needles, then $L^c \to 0$, hence $m_h \to \infty$ and $m_l \to 5/3$. Conversely, $L^c \to 1$ for high values of *a*/*c*, i.e., corresponding to thin discs. Hence, for such a morphology, both m_h and m_l tend to infinity.

Fitting Eq. (3) to the conductivity measurements was carried out by fixing the value of Φ_c, estimated from the apparent density of the grains arranged in a loose packing [3-5]. Indeed, Φ_c is slightly smaller than the packing fraction Φ_p of the percolating particles [18], in such a way that a second-order polynomial correlation between Φ_c and Φ_p may be evidenced. Since the apparent density of the uncompacted pyrolysed carbon fibres is $d_p \approx 9.5 \times 10^{-2}$ g cm^{-3}, then $\Phi_p = d_p / d_{wf} \approx 6.85 \times 10^{-2}$. The value of $\Phi_c \approx 6.14 \times 10^{-2}$ was then derived from the above polynomial correlation, corresponding to a critical density $d_c = \Phi_c \times d_{wf} \approx 8.53 \times 10^{-2}$ g cm^{-3}. Eq. (3) was then fitted to the conductivity data on the whole range of composition, see Fig. 2, leading to the following parameters : $\sigma_h \approx$ 82.7 S cm^{-1} and $t' \approx 1.431$. The value of σ_h is typical of carbonised wood-based materials (see [4] for examples), while the morphologies of both kinds of « grains » (conducting and isolating) may be derived from *t'* and Φ_c through Eq. (4)-(5). The values of the parameters m_h, m_l, L_h^c, L_l^c, and the corresponding values of the aspect ratios *a*/*c* of each phase are gathered in Table 1. The aspect ratio of the carbon particles corresponds to a ratio length to diameter of $1 / (8.29 \times 10^{-2}) \approx 12.06$. Such a value is in good agreement with what was estimated above from SEM observations. Concerning the interparticle spaces, m_l is very close to its minimum value of 3/2, thus corresponding to spherical voids. Indeed, whether the pore phase be oblate or prolate, an aspect ratio close to 1 is derived, see Table 1.

Table 1 : Morphological parameters derived from the fit of Eq. (3) to the data of Fig. 2.

Parameters	Carbon particles	Interparticle voids
m	23.31	1.52
L^c	1.518×10^{-2}	4.37×10^{-1} (oblate) or 2.21×10^{-1} (prolate)
a / c	8.29×10^{-2}	1.45 (oblate) or 6.33×10^{-1} (prolate)

Finding more or less spherical voids allows the aspect ratio of the solid grains to be directly derived from the apparent density of the carbon powder. Indeed, if the interparticle voids are spherical, it was shown from the symmetric Bruggeman model of EMT that [3] :

$$\Phi_c = \frac{9 L_h^{\,c} \left(1 - L_h^{\,c}\right)}{2 + L_h^{\,c} \left(15 - 9 L_h^{\,c}\right)} \tag{7}$$

Putting $\Phi_c \approx 6.14 \times 10^{-2}$ in (7), one finds $L_h^{\,c} \approx 1.544 \times 10^{-2}$ and hence, through (6a), $a/c \approx 8.32 \times 10^{-2}$. The latter value corresponds to a ratio length to diameter of $1 / (8.32 \times 10^{-2}) \approx 12.02$, very close to that, 12.06, found above.

PT supports both the value of the percolation threshold and that of the aspect ratio of the carbon particles. Indeed, application of Eq. (1) very close to Φ_c leads to the exponent $t \approx 1.81$, in excellent agreement with what was expected in these three-dimensional randomly disordered materials. Finally, basing again on PT, the aspect ratio of the fibre-like particles may be confirmed in an independent way. The excluded volume concept [19] indeed allows to derive lower and upper bounds for the critical volume fraction of randomly dispersed grains. The excluded volume V_e of a given object is the volume around the latter into which the centre of another similarly shaped objet brought in contact can not penetrate. In the case of percolating cylinders, the percolation threshold is linked to V_e according to :

$$1 - \exp\left(-\frac{1.4\,V}{V_e}\right) \le \Phi_c \le 1 - \exp\left(-\frac{2.8\,V}{V_e}\right), \tag{8}$$

where V is the volume of the percolating grain, and 1.4 and 2.8 are constants corresponding to randomly oriented infinitely thin rods and deformable spheres, respectively [1,19]. Since the carbon particles are thick rods, i.e., intermediate between infinitely thin rods and spheres, the actual value of Φ_c is bounded by these two limits given in Eq. (8).Condidering cylinders of length L and diameter W comprising at each end a half sphere of radius $W/2$, volume V and excluded volume V_e read [1] :

$$\begin{aligned} V &= (\pi/4)\, W^2 L + (\pi/6)\, W^3 \\ V_e &= (4\pi/3)\, W^3 + 2\pi\, W^2 L + (\pi/2)\, W L^2 \end{aligned} \tag{9}$$

The ratio length to diameter of the fibres was estimated above to be close to 12 ; putting $L = 12$ and $W = 1$ in Eq. (8)-(9), one gets $4.45 \times 10^{-2} \le \Phi_c \le 8.71 \times 10^{-2}$, in very good agreement with the previous findings.

Elastic moduli

While randomly disordered, but initially isolated, particles are forced to come closer to each other, two percolation transitions are crossed. The first one, investigated above, corresponds to the inset of a connected path all through the system. The connectivity threshold Φ_c is just below the packing fraction and, at that critical point, the system is not consolidated. The density of the packing thus needs to be higher for the particles to form a rigid network. The critical volume fraction at which the elastic modulus becomes non-zero for the first time is called the rigidity threshold, Φ_r. Hence, in such a particulate system, it is obvious that $\Phi_r > \Phi_c$, while the situation $\Phi_r = \Phi_c$ may be encountered in continuous randomly depleted systems. Anyway, above but close to Φ_r, the elastic modulus is expected to follow the percolation scaling law [11] :

$$E = E_0 \left(\Phi - \Phi_r\right)^{\tau}, \tag{10}$$

where E_0 is the elastic modulus at zero porosity and τ is the critical exponent for elasticity. Just like t, τ is universal, however its value also depends on the nature of the elastic forces acting between the contacting particles. If central forces (i.e., normal to the surface of the particles, like in most granular systems) prevail, $\tau \approx t$ in three-dimensional media, while $\tau \approx 2t$ if beam-like or angular forces control the elastic behaviour [20,21 and ref. therein]. Note that the situation $\Phi_r > \Phi_c$ is a common feature of systems in which central forces prevail over any other kind of elastic forces.

Monolithic compressed expanded graphite (EG) is another material in which the two percolation transitions, such that $\Phi_r > \Phi_c$, are met [22]. However, in contrast with the present monoliths, the consolidated blocks that can be prepared from EG do not need the presence of a binder, since the particles self interlock into each other. Since the binder is randomly dispersed among the fibre-like particles, its presence should not influence the position of the rigidity threshold, and a previous study indeed showed that various amounts of binder had only a low influence on the apparent density of the blocks [23]. Concerning compressed EG, the following relationship was evidenced for three different batches of particles [7,24] :

$$\frac{\Phi_r}{\Phi_c} = \frac{8}{5}. \tag{11}$$

Eq. (11) was justified theoretically [7] on the basis of the so-called Kirkwood-Keating model [11 and ref. therein], for which central forces are prevalent but not strictly alone. A few other elastic forces are necessary to account for the rather low rigidity threshold, i.e., only 1.6 times larger than the connectivity one according to Eq. (11). Indeed, if the forces were purely central, one should have $\Phi_r = 2(D-1)\times\Phi_c$, D being the dimensionality of the system [7 and ref. therein], and hence $\Phi_r = 4\Phi_c$ if $D = 3$. Applying this latter formula to the present monoliths leads to a rigidity threshold of 0.2455, thus corresponding to a critical density of 0.341 g cm^{-3}. Now, the lowest density investigated here, and for which the monoliths are still well consolidated, is lower : 0.3 g cm^{-3}. It is then clear that the elastic forces can not be purely central.

If Eq. (11) applies to the present monolithic materials, then $\Phi_r = 1.6\ \Phi_c \approx 9.82 \times 10^{-2}$.

Using this latter value, Eq. (10) was fitted to the elasticity data, see Fig. 3, leading to $E_0 \approx 26.2 \times 10^3$ MPa and $\tau \approx 1.83$. E_0 is in the same order of magnitude than what is usually found for many non porous carbonaceous materials [6,25], while the elasticity exponent is almost equal to the conductivity one, thus strongly supporting the prevalence of central forces within the monoliths. However, a few other kinds of forces (e.g. angular) are required and enough to lower dramatically the rigidity threshold without affecting the value of the critical exponent. Such a description of the material matches the Kirkwood-Keating model which predicts Eq. (11). While such a model was already confirmed by numerical simulations [26], it is to our knowledge only the second time that it applies to a real three-dimensional material.

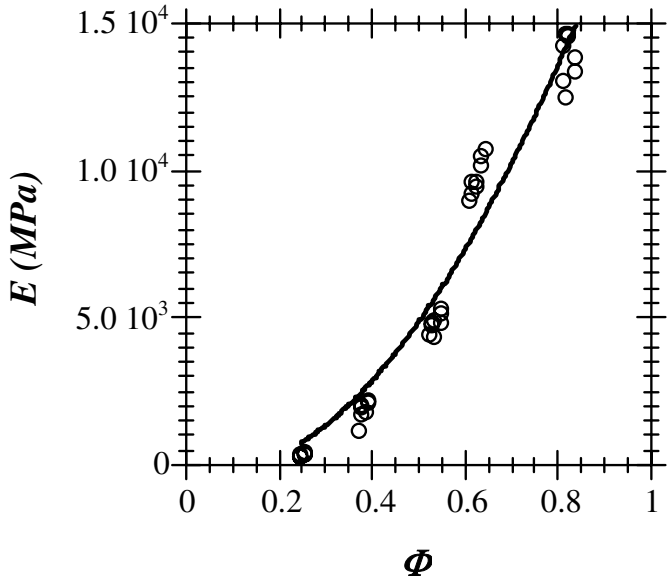

Figure 3. Elastic modulus (E) vs the volume fraction (Φ) of carbon particles. The solid curve is calculated with Eq. (10).

Conclusions

Using wood fibres and a few phenolic resin, consolidated blocks having porosities ranging from 40 to 85 % could be obtained through a simple process. Typical percolation behaviours were evidenced in such randomly disordered materials, still prolonging the extensive list of systems to which percolation theory applies. Effective-medium theory was also shown to be a useful complementary tool, enabling the accurate determination of the aspect ratios of the constituting grains and those of the interparticle voids. Finding the signature of central elastic forces through the value of the corresponding critical exponent on the one hand, and observing the relationship $\Phi_r = 8/5\ \Phi_c$ between the two critical points on the other hand, supported the relevance of the Kirkwood-Keating model. So far, the latter was only found to apply to compressed expanded graphite.

Acknowledgements

Financial support for this research came from the Deutsche Forschungsgemeinschaft (DFG).

References

[1] Celzard A, McRae E, Deleuze C, Dufort M, Furdin G, Marêché JF. Critical concentration in percolating systems containing a high-aspect-ratio filler. Phys Rev B 1996;53:6209-6214.

[2] Celzard A, Marêché JF, Payot F, Bégin D, Furdin G. Electrical conductivity of anthracites as a function of heat treatment temperature. Carbon 2000;38:1207-1215.

[3] Celzard A, Marêché JF, Payot F. Simple method for characterizing synthetic graphite powders. J Phys D Appl Phys 2000;33:1556-1563.

[4] Celzard A, Marêché JF, Payot F, Furdin G. Electrical conductivity of carbonaceous powders. Carbon 2002;40:2801-2815.

[5] Celzard A, Marêché JF, Furdin G, Puricelli S. Electrical conductivity of anisotropic expanded graphite-based monoliths. J Phys D Appl Phys 2000;33:3094-3101.

[6] Krzesiñska M, Celzard A, Marêché JF, Puricelli S. Elastic properties of anisotropic monolithic samples of compressed expanded graphite studied with ultrasounds. J Mater Res 2001;16:606-614.

[7] Celzard A, Krzesiñska M, Marêché JF, Puricelli S. Scalar and vectorial percolation in compressed expanded graphite. Physica A 2001;294:283-294.

[8] Celzard A, Marêché JF, Furdin G. J. Describing the properties of compressed expanded graphite through power laws. J Phys Condens Matter 2003;15:7213-7226.

[9] Sahimi M. Applications of Percolation Theory. Bristol PA: Taylor and Francis. 1994.

[10] Sahimi M. Flow phenomena in rocks: from continuum models to fractals, percolation, cellular automata, and simulated annealing. Rev Mod Phys 1993;65:1393-1534.

[11] Sahimi M. Non-linear and non-local transport processes in heterogeneous media: from long-range correlated percolation to fracture and materials breakdown. Phys Rep 1998;306:213-395.

[12] Fisch R, Brooks Harris A. Critical behavior of random resistor networks near the percolation threshold. Phys Rev B 1978;18:416-420.

[13] McLachlan DS. Equations for the conductivity of macroscopic mixtures. J Phys C Solid St Phys 1986;19:1339-1354.

[14] McLachlan DS. An equation for the conductivity of binary mixtures with anisotropic grain structures. J Phys C Solid St Phys 1987;20:865-877.

[15] McLachlan DS, Blaszkiewicz M, Newnham RE. Electrical resistivity of composites. J Am Ceram Soc 1990;73:2187-2203.

[16] Meredith RE, Tobias CW. Conduction in heterogeneous systems. Adv Electrochem Electrochem Eng 1962;2:15-47.

[17] Landau LD, Lifshitz EM. Electrodynamic of Continuous Media. New York: Pergamon. 1980.

[18] Ruschau GR, Newnham RE. Critical volume fractions in conductive composites. J Compos Mater 1992;26:2727-2735.

[19] Balberg I, Anderson CH, Alexander S, Wagner N. Excluded volume and its relation to the onset of percolation. Phys Rev B 1984;30:3933-3943.

[20] Sahimi M, Arbabi S. Mechanics of disordered solids. II. Percolation on elastic networks with bond-bending forces. Phys Rev B 1993;47:703-712.
[21] Del Gado E, De Arcangelis L, Coniglio A. Elastic properties at the sol-gel transition. Europhys Lett 1999;46:288-294.
[22] Celzard A, Schneider S, Marêché JF. Densification of expanded graphite. Carbon 2002;40:2185-2191.
[23] Treusch O, Hofenauer A, Tröger F, Fromm J, Wegener G. New porous carbon materials from wood-based materials. Proc. International Conf. Carbon '03 Oviedo (Spain): The Spanish Carbon Group, 2003.
[24] Celzard A, Marêché JF, Furdin G. Modelling of exfoliated graphite. Prog Mater Sci (in press)
[25] Groupe Français d'Etude des Carbones. Les Carbones. Paris: Masson. 1965.
[26] He H, Thorpe MF. Elastic Properties of Glasses. Phys Rev Lett 1985;54:2107-2110.